Electrochimica Acta 155 (2015) 341–347

Contents lists available at ScienceDirect

Electrochimica Acta

journal homepage: www.elsevier.com/locate/electacta

Target-assistant Zn^{2+}-dependent DNAzyme for signal-on electrochemiluminescent biosensing

Yin Huang, Jianping Lei *, Yan Cheng, Huangxian Ju

State Key Laboratory of Analytical Chemistry for Life Science, School of Chemistry and Chemical Engineering, Nanjing University, Nanjing 210093, PR China

ARTICLE INFO

Article history:
Received 27 October 2014
Received in revised form 27 December 2014
Accepted 31 December 2014
Available online 3 January 2015

Keywords:
Electrochemiluminescence
Quantum dots
DNAzyme
Electrocatalysis
Biosensing

ABSTRACT

A signal-on electrochemiluminescent (ECL) approach for ultrasensitive ATP detection was developed using target-assistant Zn^{2+}-dependent DNAzyme via a dual quenching pathway between quantum dots (QDs) and Au nanoclusters (Au NCs). The facile ECL biosensor was constructed by covalent assembly of Au NCs-labeled hairpin DNA on QDs modified glassy carbon electrode. A dual quenching ECL mechanism was identified to be via resonance energy transfer between QDs and Au NCs and electrocatalytic reduction of coreactant oxygen by Au NCs. With the assistance of two help DNAs, the G-quadruplex structure of ATP aptamer was formed, and thus narrowed the two fragments of Zn^{2+}-dependent DNAzyme. In the presence of Zn^{2+}, Zn^{2+}-dependent DNAzyme can be generated in situ on the biosensor's surface. The as-prepared DNAzyme can cleave the substrate strand, and release the Au NCs from the electrode, resulting in the signal-on ECL state. This biosensor showed good analytical performance with 4 orders magnitude linear range, excellent specificity, and acceptable stability. The biosensor had been applied in detection of ATP in real serum sample and provided significant potential application in clinical analysis.

1. Introduction

DNAzymes are nucleic acid-based enzymatic molecules that catalyze chemical and biological reactions including nucleic acid cleavage and peroxidase-mimicking activity [1–3]. Compared with protein enzymes, DNAzymes not only have a high catalytic ability and a good stability, but also can be easily conjugated to nanomaterials. Therefore, DNAzymes have been widely applied in sensing systems based on their catalytic ability, high specificity and effective signal transduction [4–8]. On the basis of catalytic oxidation of DNAzyme toward luminol, a multilayer hemin/G-quadruplex DNAzyme wrapped Au nanoparticle tag was designed for chemiluminescence imaging immunoassay of multiple biomarkers [4]. A DNAzyme-triggered ratiometric sensing strategy was designed to detect magnesium ion through the specific recognition toward target analyte and cleavage reaction of DNAzyme [6]. Since these methods directly replied on catalytic reaction of DNAzyme towards their corresponding substrates, the limitation of analyte range blocked their applications in practice. Here, we have designed a target-assistant DNAzyme strategy using two fragments of G-quadruplex structure to expand the applications of DNAzyme in electrochemiluminescence (ECL) biosensing.

ECL technique has received much attention in the development of the ultrasensitive detection method due to its simplicity, sensitivity and low background. In particular, quantum dots (QDs) based ECL presents an excellent prospect in detection of cells, proteins, DNAs, small biological molecules and metal ions [9–14]. The traditional ECL sensors are mainly based on three mechanisms: steric hindrance, generation/consumption of coreactant and resonance energy transfer [15–21]. Resonance energy transfer (RET) of luminol-CdSe/ZnS QDs conjugates have been applied in constructing ECL platform to monitor both conformational change of proteins and interaction between proteins [20]. A sensitive immunoassay method for biomarker detection was proposed based on ECL quenching of QDs through the annihilation of dissolved oxygen catalyzed by nitrogen-doped graphene-supported hemin [21]. However, the single quenching mechanism may easily be influenced by the complex environment of the real sample and lower the detection accuracy. Therefore, it is significant to seek a multi-quenching pathway for development of a more reliable detection method in complex samples.

Fortunately, Au nanoclusters (Au NCs) have been reported to be an energy acceptor in Au NCs-QDs RET system [22], and an excellent catalyst due to its larger specific surface area and strong quantum size effect [23]. Herein, coupling with target-assistant Zn^{2+}-dependent DNAzyme, a dual quenching ECL system of Au NCs-QDs was designed for highly specific and sensitive detection of adenosine triphosphate (ATP) (Scheme 1). Although several

* Corresponding author. Tel.: +86-25-83593593.
E-mail address: jpl@nju.edu.cn (J. Lei).

http://dx.doi.org/10.1016/j.electacta.2014.12.165
0013-4686/

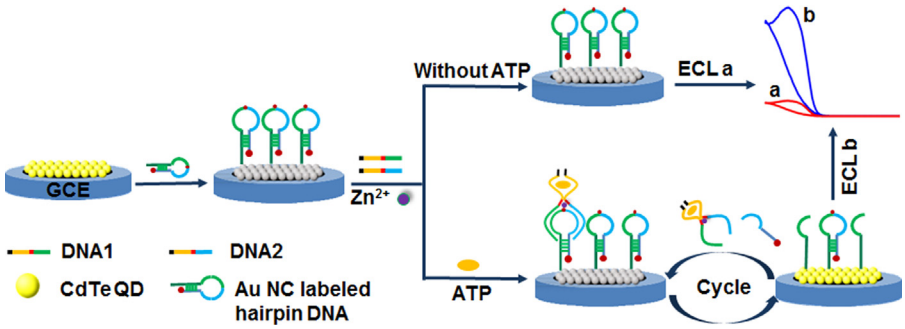

Scheme 1. Schematic illustration of signal-on ECL detection strategy of ATP based on target-assistant Zn^{2+}-dependent DNAzyme.

intriguing strategies have been developed to detect ATP, the most commonly used methods are fluorescence, colorimetric and bioluminescence for high selectivity [24–29]. In this ECL mold, an Au NCs-labeled hairpin DNA was firstly designed via Au-S bond, and then was immobilization on the surface of QDs modified glassy carbon electrode (GCE) through amide reaction. The ECL quenching mechanism was identified to be through both consumption of endogenous coreactant oxygen catalyzed by Au NCs and the RET between Au NCs and QDs. With the formation of G-quadruplex structure of ATP aptamer, a Zn^{2+}-dependent DNAzyme was in situ generated on the GCE surface. The resulting DNAzyme could cleave the substrate strand in the loop of the hairpin DNA to remove the Au NCs on the terminal, and thus the ECL signal was recovered simultaneously. This biosensor showed good analytical performance for the detection of ATP with wide linear range, excellent specificity and acceptable stability, and was successfully applied in the detection of ATP in real serum sample without any pretreatment except dilution, showing a promising application in complex samples.

2. Experimental

2.1. Materials and reagents

N-hydroxysulfosuccinimide (NHS), 1-ethyl-3-(3-dimethylaminopropyl) carbodiimide (EDC), ATP, cytidine triphosphate (CTP), uridine triphosphate (UTP), guanosine triphosphate (GTP) were purchased from Sigma-Aldrich Chemical. Co. (St. Louis, MO, U.S.A.). Meso-2, 3-dimercaptosuccinic acid (DMSA), cadmium chloride ($CdCl_2 \cdot 2.5H_2O$), 2-(N-morpholino) ethanesulfonic acid (MES) were purchased from Alfa Aesar China Ltd. (China). Isopropyl alcohol (A.R.) was purchased from Nanjing chemical reagent Co., Ltd. Tellurium rod (4 mm in diameter) was purchased from Leshan Kayada Photoelectricity Co. (China). The clinical serum sample was provided by Jiangsu Institute of Cancer Research. All other chemicals were of analytical grade and without further purification. 0.1 M pH 9.0 phosphate buffer saline (PBS) buffer solution containing 0.1 M KNO_3 as the supporting electrolyte was prepared for ECL detection. Ultrapure water ($\geq$18 MΩ, Milli-Q, Millipore) was used throughout the work.

The DNA was synthesized by Dalian Takara Biotechnology Co. Ltd. (Dalian, China). All oligonucleotides were purified by using high-performance liquid chromatography and diluted to give stock solutions in 0.1 M Tris-HCl (pH 7.4). The sequences of three oligomers are given as follows:

Hairpin DNA: 5′-NH_2-$(CH_2)_6$-AAACCACCAC AATGTTATAC AGGTACTAT rAG GAAGTTGAG TTACGAGGCG GTGGTGG-$(CH_2)_6$-SH-3′

DNA1: 5′-CTCAACTTC TCCGAGCCTGCGGAGGAAGGT-3′

DNA2: 5′-ACCTGGGGGAGTATGGTCGAA ATAGTACCT-3′

2.2. Apparatus

The synthesis of CdTe/DMSA QDs was carried out at a CHI 812B. Cyclic voltammetric (CV) and ECL experiments were performed on MPI-A multifunctional electrochemical and chemiluminescent system (Xi'an Remex Analytical Instrument Co., Ltd. China) at room temperature. A modified glassy carbon electrode (GCE, 5 mm in diameter) working electrode, a platinum wire counter electrode and a Ag/AgCl (saturated KCl) reference electrode were used in all electrochemical measurements, and all potentials were quoted against this reference electrode. Electrochemical impedance spectroscopy (EIS) measurements were carried out on a PGSTAT30/FRA2 system (Autolab, the Netherlands) in 0.1 M KNO_3 containing 5.0 mM $K_3Fe(CN)_6/K_4Fe(CN)_6$ with a frequency range of 10^{-1} to 10^{-5} Hz and an amplitude of 5.0 mV. Transmission electron microscopic (TEM) images were obtained on JEM-2100 (Japan). Dynamic light scattering (DLS) measurement was performed by BI-200SM light scattering apparatus (Brookhaven, U.S.A.).

2.3. Preparation of CdTe/DMSA QDs

According to our green electrolysis method [30], 32.9 μmol of DMSA was added into 20 mL of 0.01 M of NaOH solution and stirring about 15 min to get DMSA dissolved. After adding 120 μL 0.1 M $CdCl_2$ into the transparent solution and pumping pure N_2 for 20 min, the mixture was applied a constant potential at -1.0 V (vs. Ag/AgCl electrode) by using Te electrode as the working electrode, until the final electricity quantity reach 0.5 C with the solution turned from colourless to light brown. The solution is refluxed at 80 °C for 20 hours and stored at 4 °C before use.

2.4. Preparation of signal probe-Au NCs labelled hairpin DNA

The Au NCs were prepared according to the previous method [31]. 10 mL of 1% $HAuCl_4$ was mixed with 10 mL of 25.0 mM GSH aqueous solution by sharply stirring, and then it was kept in a dark room at 25 °C for about 2 weeks to get a light yellow solution. In order to remove the unreacted chemical substance, the solution was ultrafiltrated at 12,000 rpm for 10 min and further purification was implemented by centrifuging at 10,000 rpm for 5 min with equal volume of ethanol added. The precipitate was dissolved by vigorous ultrasound in aqueous solution and stored at 4 °C before use.

1.5 μL of 10.0 mM TCEP was added into 200 μL of 2 μM hairpin DNA in pH 7.4 Tris-HCl buffer and shacked for 1 hour to reduce disulfide bonds on the DNA. Then 200 μL of Au NCs and 2.5 μL of 10 mM MCH was mixed and shacked for 2 hours with the reduced hairpin DNA to get Au NCs-DNA through Au-S bond and it was ultrafiltrated at 12,000 rpm for 10 min and washed 3 times with

pure water to remove the unreacted substance. Then the final solution was stored at 4 °C before further use.

2.5. Fabrication of the ECL biosensor

The GCE was polished by 1.0 and 0.05 μm alumina slurry for 2 min and sonicated in dilute nitric acid, ethyl alcohol, deionized water for 2 min, respectively. 20 μL concentrated CdTe QD was dropped and dried onto the GCE naturally to form a uniform film at room temperature. Then 4 mg EDC was added and incubated at 37 °C for 30 min to activate the carboxyl of QDs. The resulting electrode was incubated with 20 μL as-prepared Au NCs-DNA at 37 °C for 2 hour and at 4 °C overnight in a 100% moisture-saturated environment.

2.6. ECL detection procedure

The electrode above was washed twice carefully with 0.1 M pH 7.4 Tris-HCl buffer containing 0.1 M NaCl to remove unbounded Au NCs-DNA, and incubated with 20 μL 0.1 μM help DNA1 and DNA2 at 37 °C for 2 h. For detecting ATP, different concentration of ATP and 0.1 mM Zn^{2+} was added together and incubated at 37 °C for 40 min. Finally, the proposed biosensor was rinsed three times and the ECL signal was detected in air-saturated 0.1 M PBS containing 0.1 M KNO_3.

3. Results and discussion

3.1. Viability of strategy

In order to prove the feasibility of the biosensor, the ECL intensity during differently modified procedure was investigated step by step. The ECL signal of the QD modified electrode was at -1.25 V was about 13,000 a.u. (Fig. 1A, curve a). After Au NCs-DNA was immobilized on the surface, an obvious decline of ECL signal was observed (Fig. 1A, curve c), which might attributed to the RET between Au NCs and the excited QDs, and the catalytical reduction of Au NCs toward oxygen as an endogenous coreactant. When adding ATP in the presence of help DNA1, DNA2 and Zn^{2+}, the Zn^{2+}-dependent DNAzyme was formed to cleave the hairpin DNAs and Au NCs was removed from the electrode surface, resulting in the recovery of ECL signal (Fig. 1A, curve b). However, in the absence of Zn^{2+}, no ECL signal change was observed (Fig. 1A, curve d). Consequently, the proposed biosensor provided an efficient method to detect ATP by ECL.

3.2. Characterization of QDs and Au NCs-DNA

High resolution TEM images are used to characterize the morphology and size of CdTe QDs (Fig. 2A) and Au NCs-DNA (Fig. 2B). The TEM image shows that CdTe QDs and Au NCs are densely arranged and monodispersed, and the average diameters of the CdTe QDs and Au NCs are 5.2 nm and 1.1 nm, respectively. After the hairpin DNA is combined with Au NCs by Au-S covalent bond, the mean hydrodynamic diameters are 1.2 and 5.8 nm for Au NCs and Au NCs-DNA, respectively (Fig. 2C, D). The difference value is almost the length of the hairpin DNA, indicating the successful synthesis of Au NCs-DNA and its well-dispersion in the aqueous solution. The outstanding water dispersibility and uniform particle size play a crucial role on the reproducibility and stability of the experiment.

3.3. Dual-quenching mechanism of ECL emission

Quenching mechanism of QDs based ECL has been reported already including destroy the structure of QDs, assumption of coreactant, and electron and energy transfer between QD and acceptor. DMSA-stabilized bidentate-chelating CdTe QDs exhibited a photoluminescence (PL) emission peak at 479 nm (λ_{ex} = 400 nm) which indicating the core band-gap emission of CdTe QDs (Fig. 3A, curve a). The UV– vis absorption spectrum of Au NCs showed an absorption shoulder peak around 470 nm (Fig. 3A, curve b) which had an excellent spectral overlap with the PL spectrum of CdTe QDs. This confirms the RET between the CdTe QDs and Au NCs [14].

On the other hand, another possible quenching pathway via electrocatalytic reduction of O_2 was identified by CVs at bare and Au CNs modified GCE [32,33]. As shown in Fig. 3B, both peak currents disappeared after bumping pure N_2 for about 5 min (Fig. 3B, curve a, c). The bare GCE showed a peak current of O_2 reduction of 6.1 μA around -0.68 V in air-saturated PBS (Fig. 3B, curve b). Meanwhile, the Au NCs modified GCE demonstrated 3 times peak current with the positive potential shift to -0.45 V (Fig. 3B, curve d), which mainly attributed to the electrocatalytic reduction of Au NCs towards O_2. This phenomenon was also confirmed at QD/Au NCs-DNA/GCE. As shown in Fig. 1B, when Au NCs-DNA immobilized on the electrode, an obviously peak current at -0.9 V was observed (Fig. 1B, curve c), which led to the consumption of O_2 and quenching of ECL. After the part removal of Au NCs-hairpin DNA via enzymatic cleavage,

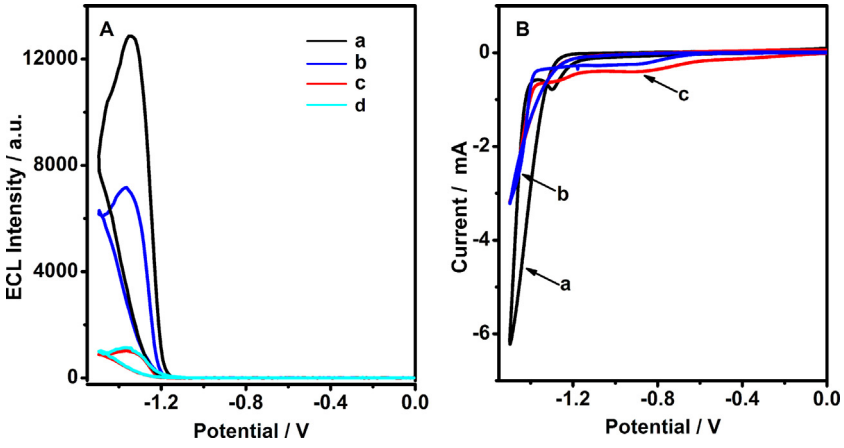

Fig. 1. (A) ECL and (B) CV response of QD/GCE (a), and QD/Au NCs-DNA/GCE with (b) and without ATP (c) in the presence of 100 nM of two help DNAs and 100 μM Zn^{2+} in air-saturated PBS. (d) is control experiment in the absence of Zn^{2+}. Scan rate: 0.1 V s^{-1}.

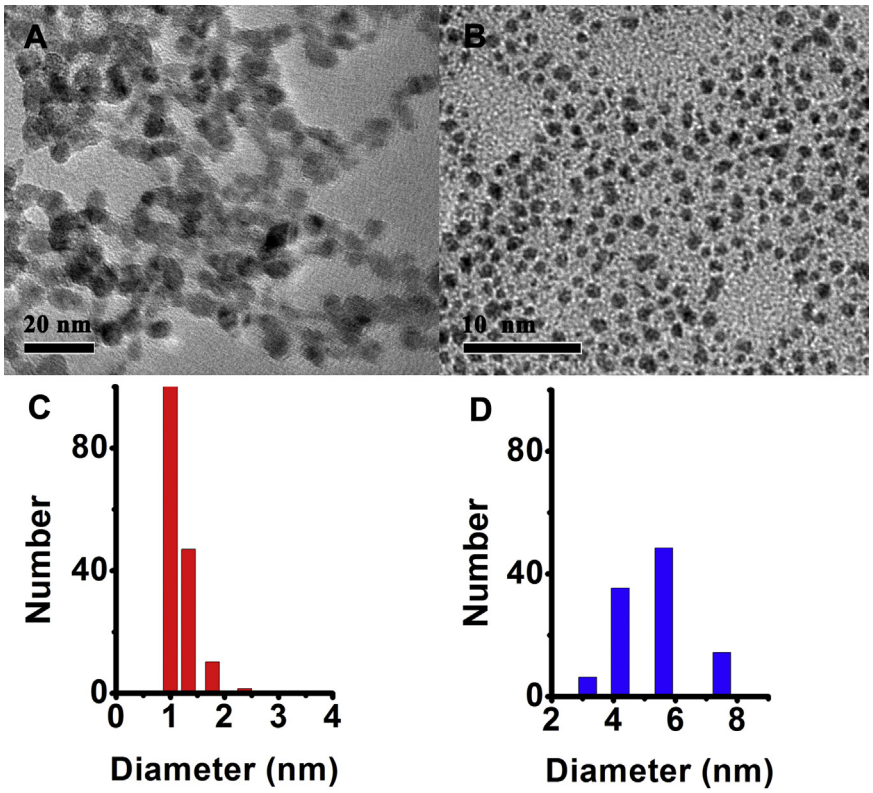

Fig. 2. High resolution TEM images of (A) CdTe QDs and (B) Au NCs, and the hydrodynamic sizes of (C) Au NCs and (D) Au NCs-DNA composite measured by DLS.

the peak potential was slightly negative moved and peak current decreased (Fig. 1B, curve b) along with the recovery of the ECL intensity (Fig. 1A, curve b), which coincided to the coreactant consumption mechanism.

3.4. Condition optimization for ECL detection

Since the CdTe QDs were ECL signal molecules, the amount of the QDs greatly affected the ECL intensity and sensitivity of the biosensor. With the increase amount of CdTe QDs, the ECL intensity increased sharply until it reached 4 nmol (Fig. 4A). Therefore, 4 nmol QDs were used throughout the following experiments. To acquire the large signal change, the amount of Au NCs-DNA was optimized. Although the lower background was obtained at the more Au NCs-DNA (Fig. 4B), the recovery efficiency of ECL was low. Thus 0.2 μM Au NCs-DNA was chosen to obtain the good sensitivity.

Meanwhile, as a Zn^{2+}-based DNAzyme induced ECL biosensor, the sensitivity of the biosensor depends on the fabrication procedure on the electrode, especially the formation and reaction of the DNAzyme. As shown in Fig. 4C, the ECL intensity reached a platform at 40 min of incubation time of ATP, indicating that the time was sufficient for cleavage reaction during the ECL detection. In addition, with the increase concentration of Zn^{2+}, the intensity of ECL enhanced sharply

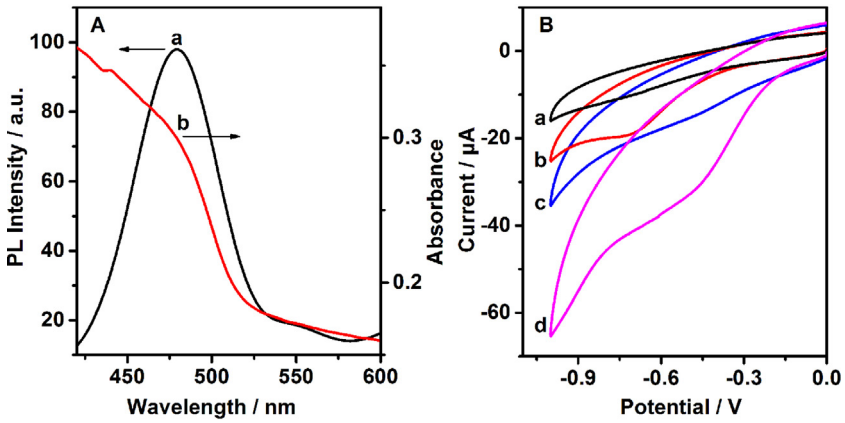

Fig. 3. (A) PL spectrum of CdTe QDs (a), UV-vis absorption of Au NCs (b). (B) CV response of GCE in N_2-saturated (a) and air-saturated PBS (b), and Au NCs/GCE in N_2-saturated (c) and air-saturated PBS (d).

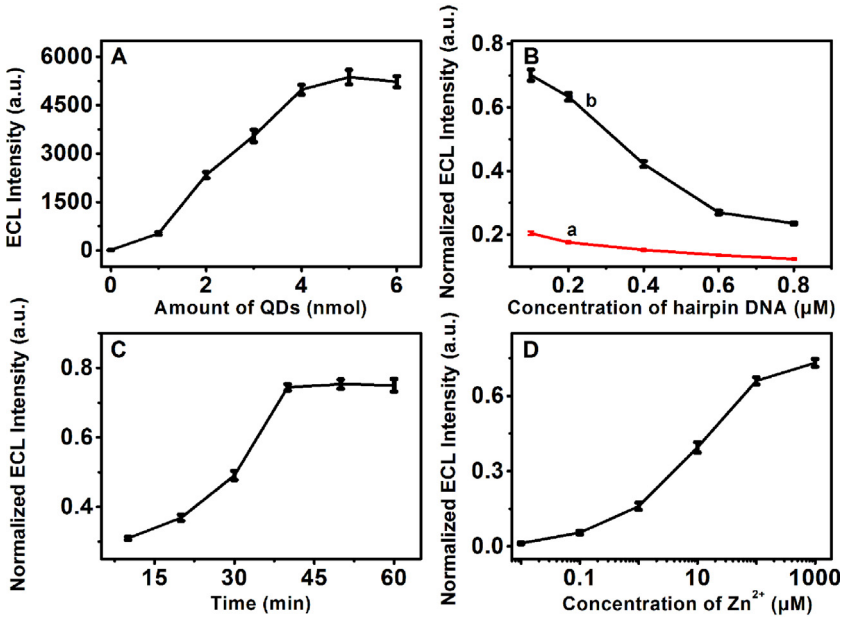

Fig. 4. Effect of the amount of (A) CdTe QDs, (B) Au NC labelled hairpin DNA before (a) and after (b) cleaving by Zn^{2+}-dependent DNAzyme, (C) incubation time of ATP and (D) concentration of Zn^{2+} on the ECL response. When one parameter is changed, the others are at their optimal value.

and remained steady above 100 μM (Fig. 4D). Thus 100 μM Zn^{2+} was favorable as the optimal concentration for this system.

3.5. Analytical performance of biosensor

The stepwise fabrication procedure of the proposed was confirmed by electrochemical impedance spectra. As shown in Fig. 5A, the bare GCE showed a quite small electron-transfer resistance (R_{ct}) around 500 Ω (curve a). Due to the intrinsic semiconductivity, the R_{ct} of CdTe QDs modified GCE was increased to ~750 Ω (curve b). After Au NCs-DNA was linked to the electrode, the R_{ct} increased sharply to 1500 Ω (curve d), which was attribute to its steric hindrance and the electrostatic repulsion between the negatively charged Au NCs-DNA and redox probe. A decrease of R_{ct} was observed (curve c) after the target ATP, Zn^{2+}, help DNA1 and DNA2 were added, because Au NCs-DNA was removed from the electrode via Zn^{2+}-dependent DNAzyme cleaving reaction.

Taking advantage of the Zn^{2+}-dependent DNAyzme, a sensitive strategy was proposed for the detection of ATP. As shown in Fig. 5B, with the increasing ATP concentration from 1 nm to 100 μM, the ECL peak intensity around -1.25 V increased regularly and a liner relationship between the ECL intensity and the logarithmic value of ATP concentration ranging from 10 nM to 50 μM, with a correlation coefficient of 0.993 (inset of Fig. 5B). The detection limit at a signal-to-noise ratio of 3 was 5.3 nM, which is lower than that of fluorescent aptasensor based on nucleic-acid functionalized silver nanoclusters hybrid system (2.5 μM) [24], and fluorescence anisotropy assay (100 nM) using DNA–protein hybrid nanowires [25].

3.6. Selectivity and stability of biosensor

The selectivity was investigated by measuring the ECL response of the proposed biosensor to CTP, UTP and GTP at the ten times concentration compared with ATP. As shown in Fig. 6A, the proposed method for ATP detection displayed 3.5 times of ECL intensity than that of the others. The high specificity was attributed to the high affinity between ATP and the aptamer, and target-assistant recognition mode. The result suggested that this detection strategy had a good prospect in the ATP analysis.

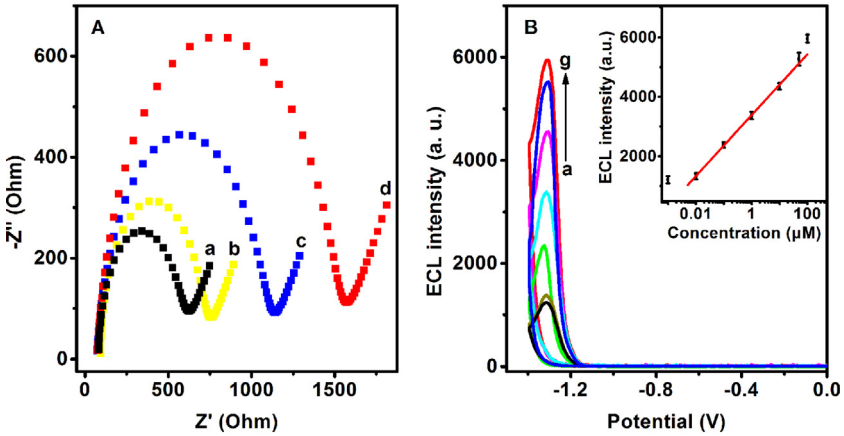

Fig. 5. (A) EIS plot of bare GCE (a), QD/GCE (b), and QD/Au NCs-DNA/GCE after (c) and before (d) cleaving by Zn^{2+}-dependent DNAzyme. (B) ECL responses of the optimized sensor to different concentrations of ATP: 0.001, 0.01, 0.1, 1, 10, 50, and 100 μM (from a to g).

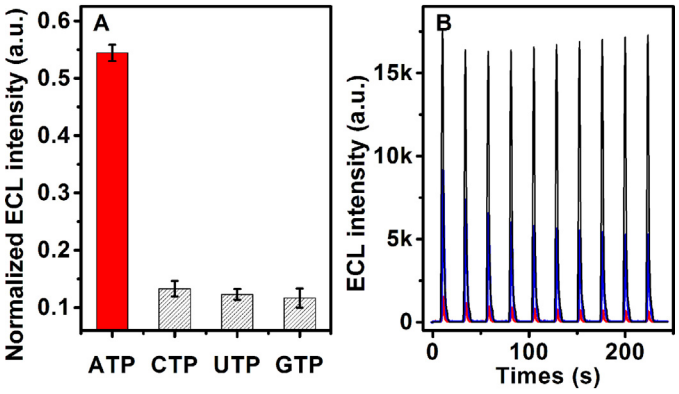

Fig. 6. (A) ECL response of the biosensor toward 1 μM ATP, and 10 μM CTP, UTP and GTP. (B) Continuous cyclic scans of QD/GCE (black), and QD/Au NCs-DNA/GCE before (red) and after (blue) cleaving by Zn^{2+}-dependent DNAzyme in air-saturated PBS.

Table 1
Detection result and recovery of ATP in serum samples.

Samples No	Add/μM	Found/μM	Recovery (%)
1	0	0.48	
	1	1.36	92.3 ± 5.2
	10	10.52	101.0 ± 6.8
2	0	0.53	
	1	1.47	93.1 ± 5.9
	10	10.37	94.2 ± 8.0

All the serum samples were not pretreated except dilution.

The proposed biosensor showed stable quenched and recovery ECL response upon continuous cyclic potential scans, indicating the feasibility for ECL detection (Fig. 6B). When the sensor was not in use, it was stored in air condition at room temperature and measured in pH 9.0 PBS every few days. No obvious change in the ECL intensity was observed after storage for 4 weeks, exhibiting a potential application in practice.

3.7. Detection of ATP in serum sample

In order to evaluate the practicability and credibility of the proposed ATP biosensor, the analysis of ATP in real serum sample was carried out without any pretreatment except dilution. Due to low concentration of ATP in the human serum samples, the low detection limit at the nanomolar level in the present biosensor was appropriate for the analysis of human serum samples. As shown in Table 1, the concentration of ATP in the different samples was calculated to be 0.48 and 0.53 μM by the standard addition method and the average recovery for the determinations ranged from 92.3 ± 5.2% and 101.0 ± 6.8%, respectively, demonstrating good accuracy for the determination of ATP in real samples. Thus, the proposed method is satisfactory for practical application in the detection of ATP for clinical diagnosis.

4. Conclusions

A "signal-on" ECL sensor for specific and sensitive detection of ATP was proposed by integrating target-assistant Zn^{2+}-dependent DNAzyme with dual-quenching ECL pathway. The ECL sensing platform was efficiently established by covalent assembly of Au-NCs probe on QDs surface. The ECL intensity of CdTe QDs was confirmed to be quenched through the electrocatalytic reduction of coreactant oxygen and energy transfer between Au NCs and CdTe QDs. With the formation of G-quadruplex structure of ATP aptamer, Zn^{2+}-dependent DNAzyme can be generated in situ on the biosensor surface. Through the efficient enzymatic cleavage reaction, the Au NCs quencher can be easily removed and ECL intensity was significantly recovered. Therefore, this strategy demonstrated the good performance of high selectivity, wide linear range, low detection limit, and a good accuracy in the application in real samples. The target-assistant DNAzyme-based detection strategy provides a promising analytical approach for complex samples and extensively expands the application of DNAzymes in bioanalysis.

Acknowledgments

We gratefully acknowledge the National Basic Research Program (2010CB732400), and National Natural Science Foundation of China (21375060, 21135002 and 21121091).

References

[1] Z.X. Zhang, D. Balogh, F. Wang, I. Willner, Smart mesoporous SiO_2 nanoparticles for the DNAzyme-induced multiplexed release of substrates, J. Am. Chem. Soc. 135 (2013) 1934.
[2] Y. Peng, L.D. Li, X.H. Yi, L. Guo, Label-free picomolar detection of Pb^{2+} using atypical icosahedra gold nanoparticles and rolling circle amplification, Biosens. Bioelectron. 59 (2014) 314.
[3] A.M. Chiorcea-Paquim, A.M. Oliver-Brett, Redox behaviour of G-quadruplexes, Electrochim. Acta 126 (2014) 162.
[4] C. Zong, J. Wu, J. Xu, H.X. Ju, F. Yan, Multilayer hemin/G-quadruplex wrapped gold nanoparticles as tag for ultrasensitive multiplex immunoassay by chemiluminescence imaging, Biosens. Bioelectron. 43 (2013) 372.
[5] S.R. Tang, W. Lu, F. Gu, P. Tong, Z.M. Yan, L. Zhang, A novel electrochemical sensor for lead ion based on cascade DNA and quantum dots amplification, Electrochimica Acta 134 (2014) 1.
[6] Y. Cheng, Y. Huang, J.P. Lei, L. Zhang, H.X. Ju, Design and biosensing of Mg^{2+}-dependent DNAzyme-triggered ratiometric electrochemiluminescence, Anal. Chem. 86 (2014) 5158.
[7] Y. Qian, C.Y. Wang, F.L. Gao, Assistant deoxyribonucleic acid recycling with Zn^{2+} and molecular beacon for electrochemical detection of deoxyribonucleic acid via target-triggered assembly of mutated DNAzyme, Anal. Chim. Acta 845 (2014) 1.
[8] P.J. Huang, J.W. Liu, Sensing parts-per-trillion Cd^{2+} Hg^{2+}, and Pb^{2+} collectively and individually using phosphorothioate DNAzymes, Anal. Chem. 86 (2014) 5999.
[9] L.L. Liu, Q. Ma, Y. Li, Z.P. Liu, X.G. Su, A novel signal-off electrochemiluminescence biosensor for the determination of glucose based on double nanoparticles, Biosens. Bioelectron. 63 (2015) 519.
[10] Y.T. Liu, J.P. Lei, Y. Huang, H.X. Ju, "Off-On" Electrochemiluminescence system for sensitive detection of ATP via target-induced structure switching, Anal. Chem. 86 (2014) 8735.
[11] S.Y. Deng, L.X. Cheng, J.P. Lei, Y. Chen, Y. Huang, H.X. Ju, Label-free electrochemiluminescent detection of DNA by hybridization with a molecular beacon to form hemin/G-quadruplex architecture for signal inhibition, Nanoscale 5 (2013) 5435.
[12] Y.Y. Chen, Y.F. Tu, The Enhanced Electrochemiluminescence of luminol by resonance energy transfer with solid-phase CdTe quantum dots, Electrochim. Acta 135 (2014) 187.
[13] W.J. Miao, Electrogenerated chemiluminescence and its biorelated applications, Chem. Rev. 108 (2008) 2506.
[14] S.Y. Deng, H.X. Ju, Electrogenerated chemiluminescence of nanomaterials for bioanalysis, Analyst 138 (2013) 43.
[15] B. Sun, H.L. Qi, F. Ma, Q. Gao, C.X. Zhang, W.J. Miao, Double covalent coupling method for the fabrication of highly sensitive and reusable electrogenerated chemiluminescence sensors, Anal. Chem. 82 (2010) 5046.
[16] F. Pinaud, L. Russo, S. Pinet, I. Gosse, V. Ravaine, N. Sojic, Enhanced electrogenerated chemiluminescence in thermoresponsive microgels, J. Am. Chem. Soc. 135 (2013) 5517.
[17] S.J. Xu, Y. Liu, T.H. Wang, J.H. Li, Positive potential operation of a cathodic electrogenerated chemiluminescence immunosensor based on luminol and grapheme for cancer biomarker detection, Anal. Chem. 83 (2011) 3817.
[18] M.S. Wu, D.J. Yuan, J.J. Xu, H.Y. Chen, Sensitive electrochemiluminescence biosensor based on Au-ITO hybrid bipolar electrode amplification system for cell Surface protein detection, Anal. Chem. 85 (2013) 11960.
[19] X.X. Zeng, S.S. Ma, J.C. Bao, W.W. Tu, Z.H. Dai, Using graphene-based plasmonic nanocomposites to quench energy from quantum dots for signal-on photoelectrochemical aptasensing, Anal. Chem. 85 (2013) 11720.
[20] L. Li, M.Y. Li, Y.M. Sun, J. Li, L. Sun, G.Z. Zou, X.L. Zhang, W.R. Jin, Electrochemiluminescence resonance energy transfer between an emitter electrochemically generated by luminol as the donor and luminescent quantum dots as the acceptor and its biological application, Chem. Commun. 47 (2011) 8292.

[21] S.Y. Deng, J.P. Lei, Y. Huang, Y. Cheng, H.X. Ju, Electrochemiluminescent quenching of quantum dots for ultrasensitive immunoassay through oxygen reduction catalyzed by nitrogen-doped graphene-supported hemin, Anal. Chem. 85 (2013) 5390.
[22] Y. Cheng, J.P. Lei, Y.L. Chen, H.X. Ju, Highly selective detection of microRNA based on distance-dependent electrochemiluminescence resonance energy transfer between CdTe nanocrystals and Au nanoclusters, Biosens. Bioelectron. 51 (2014) 431.
[23] W. Chen, S.E. Chen, Oxygen electroreduction catalyzed by gold nanoclusters: strong core size effects, Angew. Chem. Int. Ed. 48 (2009) 4386.
[24] X.Q. Liu, F. Wang, R. Aizen, O. Yehezkeli, I. Willner, Graphene oxide/nucleic-acid-stabilized silver nanoclusters: functional hybrid materials for optical aptamer sensing and multiplexed analysis of pathogenic DNAs, J. Am. Chem. Soc. 135 (2013) 11832.
[25] B. Yang, X.B. Zhang, L.P. Kang, G.L. Shen, R.Q. Yu, W.H. Tan, Target-triggered cyclic assembly of DNA-Protein hybrid nanowires for dual-amplified fluorescence anisotropy assay of small molecules, Anal. Chem. 85 (2013) 11518.
[26] Z.X. Zhang, E. Shanron, R. Freeman, X.Q. Liu, I. Willner, Fluorescence detection of DNA, adenosine-5′-triphosphate (ATP), and telomerase activity by zinc(II)-protoporphyrin IX/G-quadruplex labels, Anal. Chem. 84 (2012) 4789.
[27] H. Ahmad, B.W. Hazel, A.J.H.M. Meijer, J.A. Thomas, K.A. Wilkinson, A self-assembled luminescent host that selectively senses ATP in water, Chem. Eur. J. 19 (2013) 5081.
[28] D.H. Lee, S.Y. Kim, J.L. Hong, A fluorescent pyrophosphate sensor with high selectivity over ATP in water, Angew. Chem. Int. Ed. 43 (2004) 4777.
[29] C. Li, M. Numata, M. Takeuchi, S. Shinkai, A sensitive colorimetric and fluorescent probe based on a polythiophene derivative for the detection of ATP, Angew. Chem. Int. Ed. 44 (2005) 6371.
[30] C.W. Ge, M. Xu, J. Liu, J.P. Lei, H.X. Ju, Facile synthesis and application of highly luminescent CdTe quantum dots with an electrogenerated precursor, Chem. Commun. 4 (2008) 450.
[31] C. Zhou, C. Sun, M.X. Yu, Y.P. Qin, J.G. Wang, M. Kim, J. Zheng, Luminescent gold nanoparticles with mixed valence states generated from dissociation of polymeric Au(I) thiolates, J. Phy. Chem. C 114 (2010) 7727.
[32] S. Yamazoe, K. Koyasu, T. Tsukuda, Nonscalable oxidation catalysis of gold clusters, Acc. Chem. Res. 47 (2014) 816.
[33] K. Uosaki, G. Elumalai, H. Noguchi, T. Masuda, A. Lyalin, A. Nakayama, T. Taketsugu, Boron nitride nanosheet on gold as an electrocatalyst for oxygen reduction reaction: theoretical suggestion and experimentalproof, J. Am. Chem. Soc. 136 (2014) 6542.